DIAGNOSTIC NEURORADIOLOGY

Spatial coefficient of variation of arterial spin labeling magnetic resonance imaging can predict decreased cerebrovascular reactivity measured by acetazolamide challenge single-photon emission tomography

Naoki Taira[1] · Shoko Hara[1] · Aya Namba[1] · Yoji Tanaka[1] · Taketoshi Maehara[1]

Abstract

Purpose The aim of this study was to investigate whether the spatial coefficient of variation of arterial spin labeling (ASL-CoV) acquired in clinical settings can be used to estimate decreased cerebrovascular reactivity (CVR) measured with single-photon emission computed tomography (SPECT) and acetazolamide challenge in patients with atherosclerotic stenosis of intra- or extracranial arteries.

Methods We evaluated the data of 27 atherosclerotic stenosis patients who underwent pseudocontinuous ASL and SPECT. After spatial normalization, regional values were measured using the distributed middle cerebral artery territorial atlas of each patient. We performed comparisons, correlations, and receiver operating characteristic (ROC) curve analyses between ASL-cerebral blood blow (CBF), ASL-CoV, SPECT-CBF and SPECT-CVR.

Results Although the ASL-CBF values were positively correlated with SPECT-CBF values ($r = 0.48$, 95% confidence interval (CI) = 0.28–0.64), no significant difference in ASL-CBF values was detected between regions with and without decreased CVR. However, regions with decreased CVR had significantly greater ASL-CoV values than regions without decreased CVR. SPECT-CVR was negatively correlated with ASL-CoV ($\rho = -0.29$, 95% CI = -0.49 - -0.06). The area under the ROC curve of ASL-CoV in predicting decreased CVR (0.66, 95% CI = 0.51–0.81) was greater than that of ASL-CBF (0.51, 95% CI = 0.34–0.68). An ASL-CoV threshold value of 42% achieved a high specificity of 0.93 (sensitivity = 0.42, positive predictive value = 0.77, and negative predictive value = 0.75).

Conclusion ASL-CoV acquired by single postlabeling delay without an acetazolamide challenge may aid in the identification of patients with decreased CVR on SPECT.

Keywords Arterial spin labeling · Spatial coefficient of variation · Cerebral hemodynamics · Atherosclerotic stenosis · Cerebrovascular reactivity · Perfusion imaging

Introduction

Cerebrovascular reactivity (CVR) is an important biomarker for assessing intra- or extracranial arterial stenosis of atherosclerotic origin (AS), a cerebrovascular disorder associated with a high risk of subsequent stroke [1, 2]. CVR is the ability of the brain vasculature to increase cerebral blood flow (CBF) in response to a vasoactive stimulus. Clinically, acetazolamide (ACZ), a carbonic anhydride inhibitor, is the most widely used vasodilatation drug administered intravenously [3]. In clinical settings, CVR measurement using ACZ in single-photon emission computed tomography (SPECT) is considered the gold standard for evaluating the hemodynamics of cerebrovascular diseases. For example, the coexistence of decreased CBF and CVR is known to be a risk factor for recurrent cerebral infarction in patients with intracranial AS [4, 5]. For patients with extracranial AS, a decreased CVR is a risk factor for hyperperfusion syndrome after carotid endarterectomy or carotid artery stenting,

✉ Shoko Hara
shara.nsrg@tmd.ac.jp

1   Department of Neurosurgery, Tokyo Medical and Dental University, 1-5-45 Yushima, Bunkyo-ku, Tokyo 113-8519, Japan

even when the CBF is normal [6–9]. Therefore, although using ACZ to measure CVR is an off-label usage in Japan, CVR measurement is widely performed in clinical practice to evaluate patients with AS. However, more than half of patients experienced adverse effects from the ACZ challenge test, such as headache, nausea, dizziness, tinnitus, and numbness of the extremities. In rare and severe cases, Stevens–Johnson syndrome, life-threatening acute pulmonary edema, and reversible pontine ischemia can occur [10–13]. In addition to the side effects of ACZ, SPECT uses ionizing radiation, and SPECT scanners are not readily available in many countries. Therefore, there is an unmet need for a noninvasive method for evaluating CVR without ACZ challenge using more readily available modalities.

Arterial spin labeling magnetic resonance imaging (ASL-MRI) is a method that can noninvasively evaluate CBF by using endogenous water protons as the tracer [14]. Previous studies have reported significant correlations between the CBF measured by ASL and that measured by standard ^{15}O-gas positron emission tomography (PET-CBF) in healthy volunteers [15]. Although arterial stenosis increased arterial transit time (ATT), induced tracer arrival delay and negatively affected the CBF of ASL [14, 16, 17], a significant correlation was still observed between ASL-CBF and PET-CBF [18, 19], as well as between ASL-CBF and SPECT-CBF [20–22], in patients with AS and in patients with other intracranial arterial steno-occlusive disease or moyamoya disease (MMD). While ASL can be used to measure CVR [23] without radiation exposure, it cannot be used for direct evaluation without applying a vasoactive stimulus, and the administration of ACZ is still necessary. Several previous studies have attempted to detect CVR using ATT measured with ASL acquired via multiple postlabeling delay (PLD) methods [24]. Nevertheless, multiple PLD methods require long scanning times and complex data processing, making them difficult to apply in clinical practice [14].

Recently, the spatial coefficient of variation in ASL (ASL-CoV), which is calculated as the standard deviation (SD) divided by the average value of the signal within the region of interest (ROI), has been proposed as a novel index to evaluate hemodynamic disturbance from ASL measured with a single PLD. In patients with intra- or extracranial AS, the ATT is prolonged, and the computed CBF and CVR may be decreased. When the ATT is longer than the PLD, the labeled blood is within the vessels at the time of imaging and therefore appears as voxels with high signal intensities. At the same time, the tissue to which the labeled blood has not arrived appears dark. Therefore, the heterogeneity of the voxel values, assessed with the SD, increases, and the mean signal within the ROI decreases, resulting in high ASL-CoV in the affected areas. Therefore, AS would lead to an increase in ASL-CoV in the affected areas.

The first study that proposed ASL-CoV revealed that this index can predict ATT with relatively high precision at the single-participant level [25]. One study revealed a weak but significant correlation between ASL-CoV and CVR measured with ^{15}O-gas PET under hypercapnic conditions (r=-0.38; $p = 0.03$) in patients with AS [26]. Another study showed that ASL-CoV lateralization can predict the occlusion side in patients with unilateral carotid occlusion even in the absence of hemispheric differences in CBF [27]. In another study evaluating patients with MMD, ASL-CoV (PLD = 2500 msec) was not correlated with ASL-CVR measured with the ACZ [28]. Nevertheless, to our knowledge, few studies have measured the relationship between ASL-CoV and CVR measured with SPECT under an ACZ challenge or investigated the predictive value of ASL-CoV for decreased CVR. We hypothesized that in symptomatic patients with severe AS, the ASL-CoV is increased and negatively correlated with CVR measured with SPECT and that ASL-CoV can better predict decreased SPECT-CVR than can CBF measured with ASL. To test this hypothesis, we performed comparison, correlation, and receiver operating characteristic (ROC) curve analyses to reveal the relationships among ASL-CBF, ASL-CoV, and SPECT-CVR.

Materials and methods

This retrospective study was approved by the Tokyo Medical and Dental University ethics committee (M2017-113) and registered in the University Hospital Medical Information Network Clinical Trials Registry (UMIN-CTR ID: 000028771). We reviewed medical records and scanner examination lists from Jan 2011 to Dec 2022 and identified 27 patients with atherosclerotic intracranial arterial stenosis affecting unilateral anterior circulation who met the following inclusion criteria: (1) no prior surgical treatments before the imaging studies; (2) ASL with PLDs of both 1525 msec and 2525 msec available and SPECT performed between Jan 2011 and Dec 2022, with a time interval of less than 90 days; and (3) no new lesions or symptoms between the ASL and SPECT studies.

MRI acquisition

A 3.0-T MR scanner (GE Signa HDxt; GE Healthcare, Waukesha, WI) with an eight-channel head coil was used in this study. Two-dimensional T1 fluid-attenuated inversion recovery (FLAIR) images were acquired using the following parameters: repetition time (TR), 2139 msec; echo time (TE), 13 msec; inversion time (TI), 960 msec; echo train length, 8; slice thickness, 5.0 mm; acquisition matrix, 320×224; and field of view (FOV), 230 mm.

Two-dimensional FLAIR images were acquired using the following parameters: TR, 8800 msec; TE, 96 msec; TI, 2200 msec; ETL, 38; slice thickness, 5.0 mm; acquisition matrix, 256×160; and FOV, 230 mm. Three-dimensional pseudocontinuous ASL images were acquired using the following parameters: TR, 4521 msec; TE, 9.812 msec; FOV, 240 mm; 512 sampling points on eight spirals (matrix size, 512×8); voxel size, $1.88 \times 1.88 \times 4.0$ mm^3; number of slices, 30; number of excitations, 3; bandwidth, 62.50 Hz; and labeling time, 1.5 s. PLDs of 1525 msec and 2525 msec were acquired [29] as a tradeoff between using a long PLD to cover transit delays (a longer PLD provides a more accurate CBF [16]) and the signal-to noise ratio (a longer PLD in our clinical scanner results in poor image quality). A quantitative ASL-CBF map was generated using an Advantage Windows workstation with Functool software connected to the scanner [30]. The acquisition time for each ASL image was 4 min 22 s or 5 min 3 s depending on the PLD, and the total acquisition time of the entire MRI protocol, including FLAIR, magnetic resonance angiography, and T2-weighted imaging, was approximately 30 min.

SPECT acquisition

The subjects were injected with 222 MBq of N-isopropyl-p-[^{123}I] iodoamphetamine (^{123}I-IMP) (PERFUSAMINE: Nihon Medi-Physics, Koto-ku, Tokyo), and at 15 min after the injection, projection data were acquired using a SPECT scanner (Symbia, Siemens; Erlangen, Germany) with low- to medium-energy and general-purpose collimators, a 64×64 image matrix, a zoom factor of 1.78, 150 s per cycle, 45 views $\times$ 8 cycles and a rotating radius of 14 cm. The subjects were carefully positioned in the gamma camera using a special head-holder that allowed for a minimal rotational distance with the orbitomeatal axis in a transverse plane to avoid reorientation during reconstruction. A challenge involving the injection of 1 g of ACZ was initiated at 7–10 min before the ^{123}I-IMP injection. Radioactivity levels in the syringe and arterial blood were measured with a well counter (BASIC SCALER TDC-105: Aloka, Musashino, Tokyo) before and after the injection for accurate determination of the dose given. ^{123}I-IMP SPECT with ACZ challenge was performed within three months of the measurement of resting CBF. CBF was quantitatively measured with the IMP autoradiography method [31].

Calculation of regional values

Regional values in the proximal, middle, and distal middle cerebral artery (MCA) on ASL and SPECT images were calculated for each patient using the distributed standard atlas [32] (Fig. 1). Data processing was performed using

FreeSurfer software version 7.3.2 [33] and FMRIB Software Library (FSL) version 6.0.5.2 [34] with Lin4neuro [35]. To enhance the registration between ASL and SPECT images, superresolution 1 mm isotropic magnetization-prepared rapid acquisition with gradient echo (synthSR MPRAGE) images were synthesized from the FLAIR images using the SynthSR [36] tool in FreeSurfer software. The M0 image of ASL (ASL-M0) was coregistered to the synthSR MPRAGE of each subject via rigid transformation using FSL. The same transformation matrix used for the ASL-M0 image was applied to the ASL-CBF map, with PLDs of 1525 msec and 2525 msec. The SPECT-CBF map was also coregistered with the synthSR MPRAGE for each subject. The accuracy of the spatial registration was visually confirmed for each map. In cases where registration failed, manual registration was performed using ITK-SNAP [37]. Motion artifacts and decreased labeling efficiency due to factors such as stents were also visually confirmed for each map, as these factors can affect CBF. Subsequently, the average value of each parameter in the bilateral proximal, middle, and distal MCA areas [32] was estimated using the distributed territorial atlas (ATTbasedFlowTerritories.nii, https://figshare.com/articles/dataset/ATT_based_flow_territories/1488674). The atlas was coregistered with the synthSR MPRAGE by calculating the inverse transformation matrix for the synthSR MPRAGE to the Montreal Neurological Institute space using FSL. This calculation involved both affine and non-linear transformations to obtain an isotropic voxel size of 2 mm.

All regional ASL-CBF and SPECT-CBF values were normalized to the values of the contralateral ROI. The SD of ASL within each region was also obtained. The ASL-CoV of each ROI was calculated as the SD divided by the average of each ROI [25]:

$$ASL - CoV \, [\%] = 100 * \frac{SD_{ASL-CBF}}{Mean_{ASL-CBF}}$$

where $SD_{ASL-CBF}$ and $Mean_{ASL-CBF}$ represent the SD and mean value of the ASL-CBF map within each ROI, respectively.

The SPECT-CVR of each ROI was calculated as the change in CBF after the administration of ACZ compared with the baseline CBF [38]:

$$SPECT - CVR \, [\%] = 100 * \frac{CBF_{ACZ} - CBF_{rest}}{CBF_{rest}}$$

where CBF_{rest} and CBF_{ACZ} represent the CBF values before and after intravenous injection of acetazolamide, respectively.

Fig. 1 A representative case and the image pipeline used in this study. A 46-year-old male who initially presented with right-sided hemiparalysis was referred to our institution after his symptoms improved following acute treatment for ischemia. Magnetic resonance angiography revealed left internal carotid artery occlusion, and fluid-attenuated inversion recovery (FLAIR) images revealed a minor chronic ischemic lesion in the basal ganglia. Arterial transit artifacts on cerebral blood flow maps of arterial spin labeling (ASL-CBF) are evident in the left hemisphere. Decreased CBF is more evident in the ASL-CBF map with a postlabeling delay (PLD) = 1525 msec than in the ASL-CBF map with a PLD = 2525 msec. CBF maps of single-photon emission computed tomography (SPECT-CBF) at rest and after the acetazolamide (ACZ) challenge test indicate decreased CBF and cerebrovascular reactivity (CVR). For region-of-interest (ROI) analysis, magnetization-prepared rapid acquisition with gradient echo images were synthesized from 2D FLAIR images and used as a reference for ASL M0 images, SPECT-CBF maps and standard template regions of interest (ROIs). ASL-CBF maps were coregistered by using the transformation matrix of ASL M0 images.
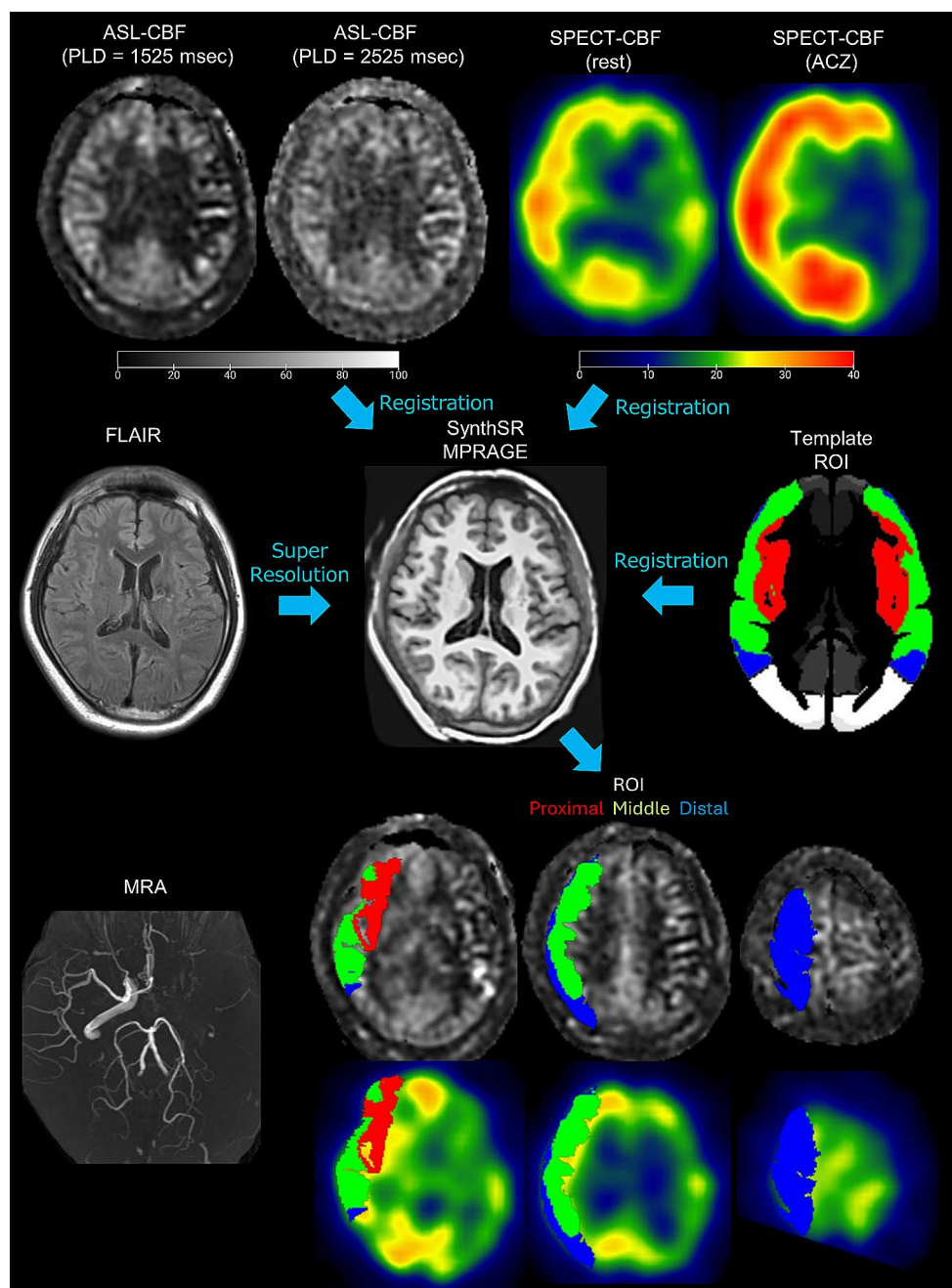
Statistical analysis

Statistical analysis was performed with R version 4.3.2 [39]. A significance level of $P < 0.05$ was considered statistically significant. In the case of multiple comparisons, the significance level was corrected via the Bonferroni method. According to previous studies, decreased CBF was defined as CBF < 80% [40, 41], and decreased CVR was defined as CVR < 10% [40, 42, 43]. To ensure the accuracy of the analysis of viable brain tissues, we excluded ROIs that were categorized as infarcted lesions with oxygen hypometabolism,

i.e., type 4 lesions with decreased CBF and normal CVR [4, 44, 45].

First, the normality of the distribution of each value was evaluated with the Shapiro–Wilk test. The values were compared for each PLD of ASL-CBF and ASL-CoV, as were the SPECT-CBF values in regions with either decreased or non-decreased CVR. If the data were suspected to be normally distributed, Welch's t test and Pearson's product moment correlation coefficient were used; if not, the Wilcoxon rank-sum test and Spearman's rank correlation coefficient were used. Correlations between each PLD of ASL-CBF and ASL-CoV, SPECT-CBF, and CVR in each region were

Table 1 Patient characteristics

	$N = 27$
Age	66 (50, 73)
Sex	
Male	20 (74%)
Lesion Side	
Left	16 (59%)
Lesion	
Internal Carotid Artery	9 (33%)
Middle Cerebral Artery	18 (67%)
Symptom	
Transient Ischemic Attack	7 (26%)
Cerebral Infarction	20 (74%)
Hypertension	19 (70%)
Diabetes Mellitus	8 (30%)
Dyslipidemia	19 (70%)

Values are the median (interquartile range) or n (%)

calculated. The strength of the correlations is described via the Evans classification [46]. Additionally, the ROC curve predicting decreased CVR was calculated for each PLD of both ASL-CBF and ASL-CoV, and differences in the areas under the ROC curve (AUCs) between ASL-CoV and ASL-CBF at each PLD were assessed. Their significance was evaluated via a bootstrap test with 2000 resampling iterations. In this analysis, due to multiple comparisons, the significance level was adjusted to $P < 0.0125$. The optimal cutoff value was determined using the Youden index [47], after which the sensitivity, specificity, positive predictive value (PPV), and negative predictive value (NPV) were computed.

Results

A total of 27 patients were included in this study. Registration between MRI and SPECT using FSL failed in 7 patients and required manual registration with ITK-SNAP. No patients were excluded due to motion artifacts or a reduced labeling efficiency. A summary of the patients' characteristics is given in Table 1. For patients with cerebral infarction symptoms, the median durations from onset to MRI and SPECT acquisition were 56 days (interquartile range (IQR): 39.5, 1069 days) and 80 days (IQR: 47.75, 1050.75 days), respectively. The extended duration between MRI and SPECT was due mainly to the limited availability of the SPECT scanner at our institute (once a week). Among the 81 ipsilateral ROIs in the 27 patients, 11 ROIs were excluded because they exhibited decreased SPECT-CBF and normal SPECT-CVR and were presumed to be infarcted lesions with oxygen hypometabolism. Thus, a total of 70 ipsilateral ROIs were included in the analysis. Among the 70 ROIs analyzed, 4 (5.7%) showed decreased SPECT-CBF,
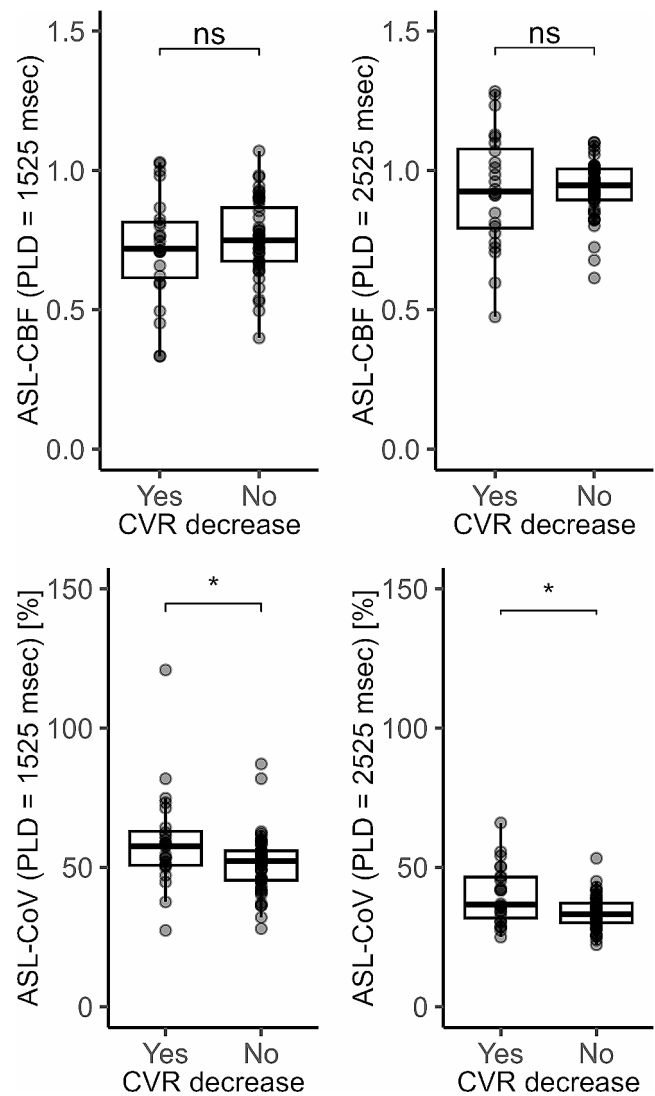

Fig. 2 Regional values of arterial spin labeling cerebral blood flow (ASL-CBF) and coefficient of variation (ASL-CoV) in regions of interest with and without decreased cerebrovascular reactivity (CVR). While ASL-CBF values were not significantly different between the two groups, ASL-CoV values were significantly greater in the regions with decreased CVR. ns: not significant, *$P < 0.05$ (Welch's t test for ASL-CBF and Wilcoxon rank sum test for ASL-CoV)

and 24 (34%) showed decreased SPECT-CVR. Parametric maps of a representative patient and ROIs in this study are shown in Fig. 1. Because the values of ASL-CoV at both PLDs and SPECT-CVR did not follow a normal distribution ($P < 0.01$), nonparametric analysis was utilized to evaluate these values.

When comparing ROIs with and without decreased SPECT-CVR, there was no difference in ASL-CBF values, but ASL-CoV values were significantly greater for ROIs with decreased SPECT-CVR (Fig. 2). ASL-CBF showed a moderate positive correlation with SPECT-CBF at both PLDs (Fig. 3). Furthermore, while ASL-CBF did not
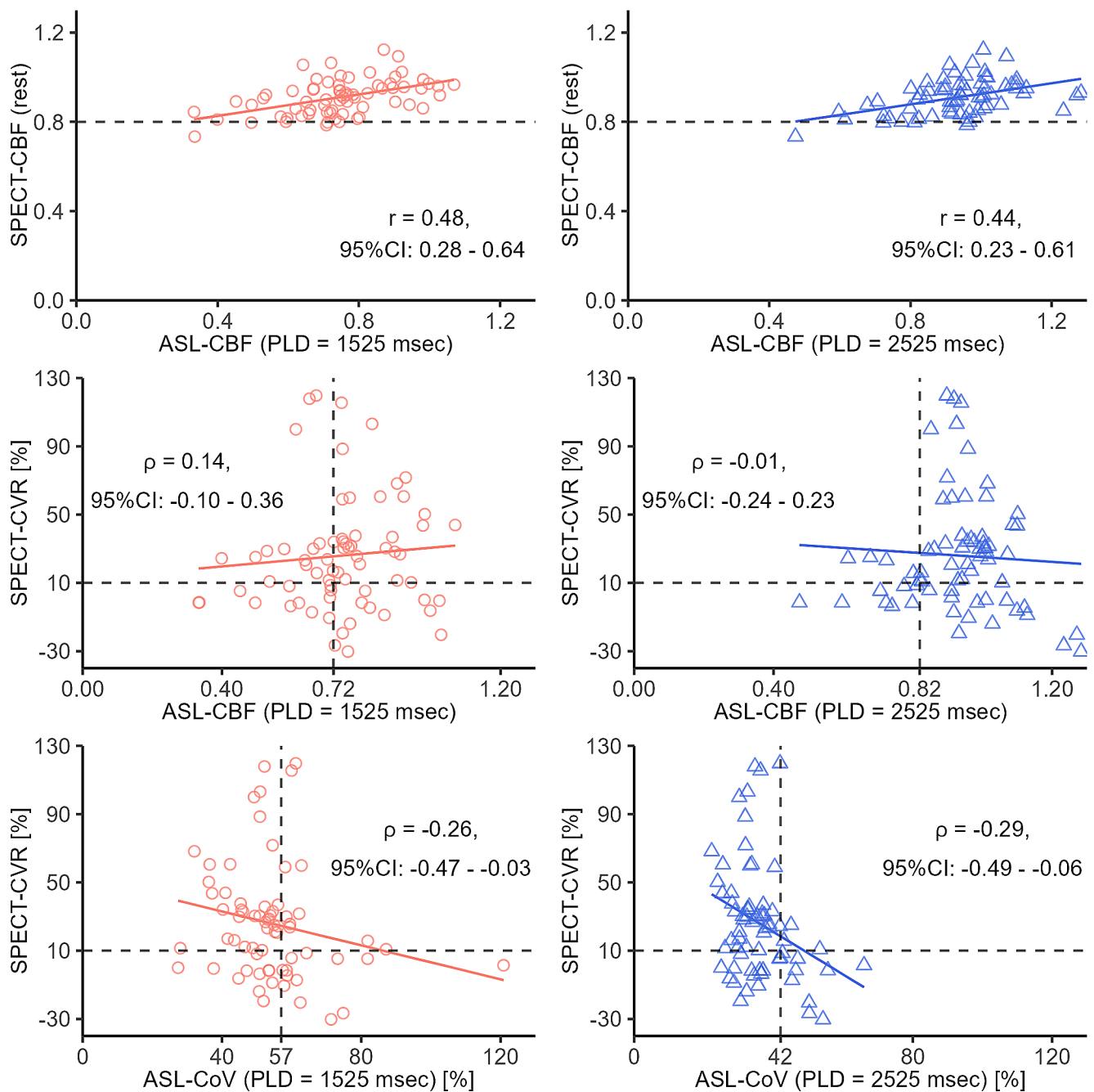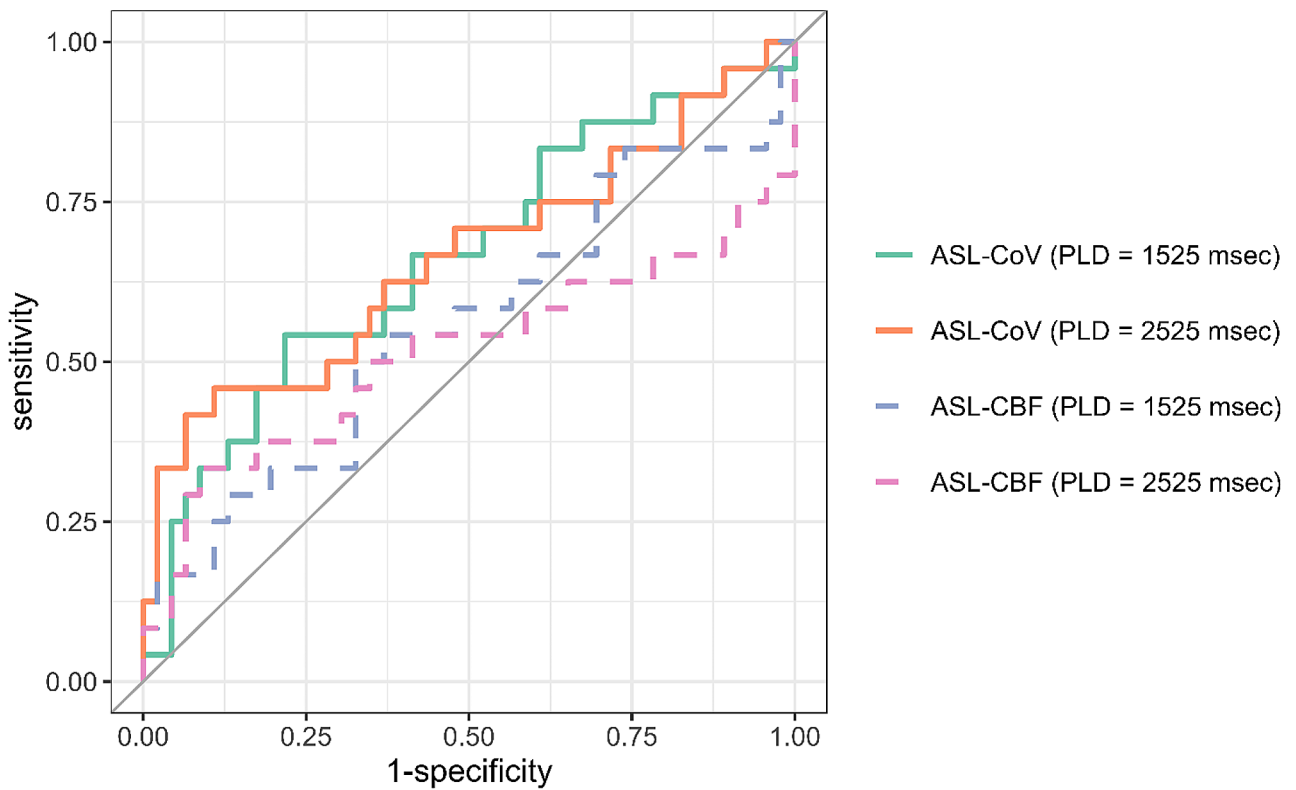
Fig. 3 Correlation analysis of cerebral blood flow (CBF) and the coefficient of variation (CoV) measured by arterial spin labeling (ASL) and CBF and cerebrovascular reactivity (CVR) measured by single-photon emission computed tomography (SPECT). ASL-CBF demonstrated a moderate positive correlation with SPECT-CBF at both PLDs (upper row) but showed no correlation with SPECT-CVR (middle row). On the other hand, ASL-CoV demonstrated a weak negative correlation with SPECT-CVR at both PLDs (lower row). In each graph, the horizontal dashed line indicates the borderline of decreased SPECT-CBF and SPECT-CVR, and the vertical dashed line indicates the optimal threshold of ASL-derived parameters determined by the Youden index of receiver operating characteristic curve analysis. 95% CI: 95% confidence interval

correlate with SPECT-CVR, ASL-CoV showed a weak negative correlation with SPECT-CVR at both PLDs (Fig. 3). In the ROC analysis, the highest AUC value was observed for ASL-CoV (PLD = 2525 msec). For both PLDs, although it was not statistically significant, the AUC of ASL-CoV was greater than that of ASL-CBF, with a 95% confidence interval (CI) lower limit above 0.5 (Fig. 4). At a cutoff value of 57%, ASL-CoV (PLD = 1525 msec) had the highest sensitivity and NPV between itself and ASL-CBF (Fig. 4). At a cutoff value of 42%, ASL-CoV (PLD = 2525 msec)

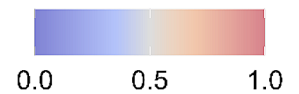|	AUC	Threshold	Sensitivity	Specificity	PPV	NPV
ASL-CoV (PLD = 1525ms)	0.66 (0.52 – 0.80)	57	0.54	0.78	0.57	0.77
ASL-CoV (PLD = 2525ms)	0.66 (0.51 – 0.81)	42	0.42	0.93	0.77	0.75
ASL-CBF (PLD = 1525ms)	0.56 (0.40 – 0.71)	0.72	0.50	0.67	0.44	0.72
ASL-CBF (PLD = 2525ms)	0.51 (0.34 – 0.68)	0.82	0.33	0.91	0.67	0.72

Fig. 4 Receiver operating characteristic analysis of cerebral blood flow (CBF) and the coefficient of variation (CoV) measured with arterial spin labeling (ASL) to predict decreased cerebrovascular reactivity (CVR). ASL-CoV had the highest area under the receiver operating characteristic curve (AUC) for both postlabeling delays (PLDs). The background of each probability value and AUC value is color-coded with a gradient from blue to red, corresponding to the respective values. AUC: area under the receiver operating characteristic curve, PPV: positive predictive value, NPV: negative predictive value, PLD: postlabeling delay, 95% CI: 95% confidence interval

exhibited the highest specificity and PPV between itself and ASL-CBF.

Discussion

In this study, we found that regions with decreased CVR had higher values of ASL-CoV and that CVR was negatively correlated with ASL-CoV. According to ROC curve analysis, the AUC of ASL-CoV in predicting a decreased CVR was greater than that of ASL-CBF for both PLDs. ASL-CoV (PLD = 2525 msec) had the highest AUC, specificity and PPV. Our ASL protocol and routine MR sequences can be acquired within 30 min and are clinically feasible.

ASL-CoV was weakly correlated with SPECT-CVR for both PLDs, whereas ASL-CBF did not show a correlation with SPECT-CVR. The correlation coefficients between ASL-CoV and SPECT-CVR were similar to those reported in a previous ^{15}O-gas PET study ($|r|$=0.38), in which CVR was evaluated under hypercapnic conditions [26]. Our study employed a novel CVR quantification method that uses SPECT with ACZ, which has well-established clinical importance [6–9]. Theoretically, as stenosis progresses and cerebral perfusion pressure (CPP) decreases, the increase in the mean transit time (MTT) and cerebral blood volume (CBV) begins before the CBF decreases [48]. At this point, CVR also starts to decrease, while CBF is maintained. As the CPP continues to decrease, the CBF starts to decrease. The lack of correlation between CBF and CVR is therefore reasonable [24, 49]. In a previous study evaluating patients with MMD, ASL-CoV showed a moderate to strong ($|r|$=0.63–0.80) correlation between CBV and MTT measured with ^{15}O-gas PET, but the correlations between ASL-CBF, CBV and MTT were weak, as in our study [18, 29]. ASL-CoV might be negatively correlated with CVR because of the increased SD within the ROIs in AS patients. As we stated in the Introduction section, in the case of arterial stenosis, the prolonged ATT can cause some tissue voxels in which labeled protons have not yet arrived to have low values. Moreover, other voxels with delayed arrivals of labeled protons produce increased intensities because at the time of imaging, labeled protons were still present in the cortical arteries, including the leptomeningeal collaterals [19, 50]. In another study of patients with MMD, ASL-CoV (PLD = 2500 msec) did not correlate with ASL-CVR measured with ACZ [28]. This difference from our study results may be due to the different pathophysiologies of MMD and AS. In patients with MMD, which is characterized by a very long ATT and arterial transit artifacts reflecting leptomeningeal collaterals [16, 51], the correlation between ASL-CBF (PLD = 2525 msec) and true CBF measured with ^{15}O-PET was not as strong as the correlation observed in patients with

AS [19]. Therefore, it is possible that the ASL-CVR was negatively affected by poor quantification of CBF in MMD patients and therefore did not correlate with ASL-CoV.

The AUC in detecting a decrease in CVR caused by ASL-CoV was greater than that of ASL-CBF. Although there was no statistically significant relationship between ASL-CoV and ASL-CBF, only ASL-CoV had a lower limit of the 95% CI above 0.5 for both PLDs. This result suggests that ASL-CoV may be a more reliable indicator for detecting a decrease in CVR than ASL-CBF is. The AUC values for ASL-CoV were equal for PLDs of both 1525 msec and 2525 msec (0.66 vs. 0.66). When the cutoff value of ASL-CoV was set at 57% (PLD = 1525 msec) and 42% (PLD = 2525 msec), although ASL-CoV (PLD = 2525 msec) had a lower sensitivity than ASL-CoV (PLD = 1525 msec; 0.42 vs. 0.52), it had greater specificity (0.93 vs. 0.78), a greater PPV (0.77 vs. 0.57) and a similar high NPV (0.75 vs. 0.77). When applying ASL-CoV as a screening method for detecting decreased CVR, ASL-CoV (PLD = 2525 msec) seems more suitable than ASL-CoV (PLD = 1525 msec) because of its higher specificity and similar NPV. A high NPV suggests that if ASL-CoV (PLD = 2525 msec) is below the threshold, CVR is likely to be normal. If we can restrict ACZ challenge only for cases of ASL-CoV above the threshold value, the number of patients who require invasive ACZ would greatly decrease. This will not only decrease patients' physical burden but also reduce healthcare costs, which are rapidly increasing in Japan.

ASL-CBF showed a moderate correlation with SPECT-CBF for both PLDs (ρ = 0.48, 0.44). This result is likely because ASL-CBF was underestimated with a single PLD method in AS patients who had an elongated ATT [14]. A previous study reported a stronger correlation [20], but the ASL sequence used in this study is not currently available in clinical settings. The characteristics of this study include the use of single PLD pseudocontinuous ASL, which has a shorter scanning time and utilizes CBF maps calculated within the scanner, making it readily available for clinicians. Considering the results of ASL-CoV, ASL-CBF (PLD = 2525 msec) might be more suitable in clinical practice. Theoretically, a longer PLD is considered appropriate for populations with a high proportion of elderly individuals [52]. Although the number of patients with decreased CBF was small and the ability of ASL-CBF to detect decreased SPECT-CBF could not be evaluated in this study, if ASL-CBF can detect decreased SPECT-CBF, it would also be beneficial for patients by reducing their exposure to radiation.

The limitations of this study include its retrospective, single-center design and small sample size. The interval between SPECT studies at rest and the ACZ challenge, as well as the ASL-SPECT interval, was relatively long due

to the limited availability of SPECT examinations at our institution. The lack of comparative data from healthy controls is another limitation. Even when the same PLD and pseudocontinuous ASL or IMP-SPECT with autoradiography quantification are used, the results cannot be applied to different institutes without verification. Overall, the results might be affected by the small number of regions with reduced CBF and CVR.

Despite these limitations, our study demonstrated that ASL-CoV measured at a single PLD correlates with SPECT-CVR in patients with AS and has the potential to predict decreased CVR without ACZ challenge. Because of the high specificity and NPV, normal CVR is likely when the ASL-CoV values are below the threshold; thus, we can potentially avoid SPECT with an ACZ challenge for such patients. Prospective validation of our study is needed in the future.

Declarations

Disclosures Dr. Yoji Tanaka has received a donation from Kyowa Kirin Pharmaceutical Development for education and research. The rest of the authors have nothing to disclose.

Ethical approval All procedures performed in the studies involving human participants were in accordance with the ethical standards of the institutional and/or national research committee and with the 1964 Helsinki Declaration and its later amendments or comparable ethical standards.

Informed consent Informed consent was obtained from all individual participants included in the study.

References

1. Kasner SE, Chimowitz MI, Lynn MJ, Howlett-Smith H, Stern BJ, Hertzberg VS et al (2006) Predictors of ischemic stroke in the Territory of a symptomatic intracranial arterial stenosis. Circulation 113:555–563. https://doi.org/10.1161/CIRCULATIONAHA.105.578229
2. Flaherty ML, Flemming KD, McClelland R, Jorgensen NW, Brown RD Jr (2004) Population-based study of symptomatic internal carotid artery occlusion: incidence and long-term follow-up. Stroke 35:e349–352. https://doi.org/10.1161/01.STR.0000135024.54608.3f
3. Bonte FJ, Devous MD, Reisch JS (1988) The effect of acetazolamide on regional cerebral blood flow in normal human subjects as measured by single-photon emission computed tomography. Invest Radiol 23:564–568. https://doi.org/10.1097/00004424-198808000-00003
4. Kuroda S, Houkin K, Kamiyama H, Mitsumori K, Iwasaki Y, Abe H (2001) Long-term prognosis of medically treated patients with internal carotid or middle cerebral artery occlusion: can acetazolamide test predict it? Stroke 32:2110–2116. https://doi.org/10.1161/hs0901.095692
5. Ogasawara K, Ogawa A, Yoshimoto T (2002) Cerebrovascular reactivity to acetazolamide and outcome in patients with symptomatic internal carotid or middle cerebral artery occlusion: a xenon-133 single-photon emission computed tomography study. Stroke 33:1857–1862. https://doi.org/10.1161/01.str.0000019511.81583.a8
6. Kaku Y, Yoshimura S, Kokuzawa J (2004) Factors predictive of cerebral hyperperfusion after carotid angioplasty and stent placement. AJNR Am J Neuroradiol 25:1403–1408
7. Oshida S, Ogasawara K, Saura H, Yoshida K, Fujiwara S, Kojima D et al (2015) Does preoperative measurement of cerebral blood flow with acetazolamide challenge in addition to preoperative measurement of cerebral blood flow at the resting state increase the predictive accuracy of development of cerebral hyperperfusion after carotid endarterectomy? Results from 500 cases with brain perfusion single-photon emission computed tomography study. Neurol Med Chir (Tokyo) 55:141–148. https://doi.org/10.2176/nmc.oa.2014-0269
8. Hosoda K, Kawaguchi T, Shibata Y, Kamei M, Kidoguchi K, Koyama J et al (2001) Cerebral vasoreactivity and internal carotid artery flow help to identify patients at risk for hyperperfusion after carotid endarterectomy. Stroke 32:1567–1573. https://doi.org/10.1161/01.str.32.7.1567
9. Ogasawara K, Yukawa H, Kobayashi M, Mikami C, Konno H, Terasaki K et al (2003) Prediction and monitoring of cerebral hyperperfusion after carotid endarterectomy by using single-photon emission computerized tomography scanning. J Neurosurg 99:504–510. https://doi.org/10.3171/jns.2003.99.3.0504
10. Zimmermann S, Achenbach S, Wolf M, Janka R, Marwan M, Mahler V (2014) Recurrent shock and pulmonary edema due to acetazolamide medication after cataract surgery. Heart Lung 43:124–126. https://doi.org/10.1016/j.hrtlng.2013.11.008
11. Vogiatzis I, Koulouris E, Sidiropoulos A, Giannakoulas C (2013) Acute pulmonary edema after a single oral dose of acetazolamide. Hippokratia 17:177–179
12. Mugikura S, Fujimura M, Takahashi S (2016) Implications of off-label use of Acetazolamide in the management of Moyamoya Disease in Japan. Radiology 279:652–653. https://doi.org/10.1148/radiol.2016152305
13. Komiyama M, Nishikawa M, Yasui T, Sakamoto H (1997) Reversible pontine ischemia caused by acetazolamide challenge. AJNR Am J Neuroradiol 18:1782–1784
14. Alsop DC, Detre JA, Golay X, Gunther M, Hendrikse J, Hernandez-Garcia L et al (2015) Recommended implementation of arterial spin-labeled perfusion MRI for clinical applications: a consensus of the ISMRM perfusion study group and the European consortium for ASL in dementia. Magn Reson Med 73:102–116. https://doi.org/10.1002/mrm.25197
15. Puig O, Henriksen OM, Vestergaard MB, Hansen AE, Andersen FL, Ladefoged CN et al (2020) Comparison of simultaneous arterial spin labeling MRI and 15O-H2O PET measurements of regional cerebral blood flow in rest and altered perfusion states. J Cereb Blood Flow Metabolism 40:1621–1633. https://doi.org/10.1177/0271678x19874643
16. Fan AP, Guo J, Khalighi MM, Gulaka PK, Shen B, Park JH et al (2017) Long-Delay arterial spin labeling provides more Accurate Cerebral Blood Flow measurements in Moyamoya patients: a simultaneous Positron Emission Tomography/MRI Study. Stroke 48:2441–2449. https://doi.org/10.1161/strokeaha.117.017773
17. Wang J, Alsop DC, Song HK, Maldjian JA, Tang K, Salvucci AE et al (2003) Arterial transit time imaging with flow encoding arterial spin tagging (FEAST). Magn Reson Med 50:599–607. https://doi.org/10.1002/mrm.10559

18. Hara S, Tanaka Y, Ueda Y, Hayashi S, Inaji M, Ishiwata K et al (2017) Noninvasive evaluation of CBF and Perfusion Delay of Moyamoya Disease using arterial spin-labeling MRI with multiple postlabeling delays: comparison with (15)O-Gas PET and DSC-MRI. AJNR Am J Neuroradiol 38:696–702. https://doi.org/10.3174/ajnr.A5068

19. Ueda Y, Tanaka Y, Hara S, Inaji M, Ishii K, Maehara T et al (2023) Differences in cerebral blood flow measurement using arterial spin labeling MRI between patients with moyamoya disease and patients with arteriosclerotic cerebrovascular disease. Acta Radiol 64:311–319. https://doi.org/10.1177/02841851211069245

20. Uchihashi Y, Hosoda K, Zimine I, Fujita A, Fujii M, Sugimura K et al (2011) Clinical application of arterial spin-labeling MR imaging in patients with carotid stenosis: quantitative comparative study with single-photon emission CT. AJNR Am J Neuroradiol 32:1545–1551. https://doi.org/10.3174/ajnr.A2525

21. Noguchi T, Kawashima M, Irie H, Ootsuka T, Nishihara M, Matsushima T et al (2011) Arterial spin-labeling MR imaging in Moyamoya disease compared with SPECT imaging. Eur J Radiol 80:e557–562. https://doi.org/10.1016/j.ejrad.2011.01.016

22. Setta K, Matsuda T, Sasaki M, Chiba T, Fujiwara S, Kobayashi M et al (2021) Diagnostic accuracy of screening arterial spin-labeling MRI using Hadamard Encoding for the detection of reduced CBF in Adult patients with ischemic Moyamoya Disease. AJNR Am J Neuroradiol 42:1403–1409. https://doi.org/10.3174/ajnr.A7167

23. Zhao MY, Václavů L, Petersen ET, Biemond BJ, Sokolska MJ, Suzuki Y et al (2020) Quantification of cerebral perfusion and cerebrovascular reserve using Turbo-QUASAR arterial spin labeling MRI. Magn Reson Med 83:731–748. https://doi.org/10.1002/mrm.27956

24. Choi HJ, Sohn CH, You SH, Yoo RE, Kang KM, Yun TJ et al (2018) Can arterial spin-labeling with multiple postlabeling delays predict Cerebrovascular Reserve? AJNR Am J Neuroradiol 39:84–90. https://doi.org/10.3174/ajnr.A5439

25. Mutsaerts HJ, Petr J, Vaclavu L, van Dalen JW, Robertson AD, Caan MW et al (2017) The spatial coefficient of variation in arterial spin labeling cerebral blood flow images. J Cereb Blood Flow Metab 271678X:16683690. https://doi.org/10.1177/0271678X16683690

26. Ibaraki M, Nakamura K, Toyoshima H, Takahashi K, Matsubara K, Umetsu A et al (2019) Spatial coefficient of variation in pseudo-continuous arterial spin labeling cerebral blood flow images as a hemodynamic measure for cerebrovascular steno-occlusive disease: a comparative (15)o positron emission tomography study. J Cereb Blood Flow Metab 39:173–181. https://doi.org/10.1177/0271678X18781667

27. Mutsaerts H, Petr J, Bokkers RPH, Lazar RM, Marshall RS, Asllani I (2020) Spatial coefficient of variation of arterial spin labeling MRI as a cerebrovascular correlate of carotid occlusive disease. PLoS ONE 15:e0229444. https://doi.org/10.1371/journal.pone.0229444

28. Fahlström M, Svedung Wettervik T, Enblad P, Lewén A, Wikström J (2023) Evaluation of single-delay arterial spin labeling-based spatial coefficient of variation and histogram-based parameters in relation to cerebrovascular reserve in patients with Moyamoya disease. Front Neurol 14. https://doi.org/10.3389/fneur.2023.1137046

29. Hara S, Tanaka Y, Inaji M, Hayashi S, Ishii K, Nariai T et al (2022) Spatial coefficient of variation of arterial spin labeling MRI for detecting hemodynamic disturbances measured with (15)O-gas PET in patients with moyamoya disease. Neuroradiology 64:675–684. https://doi.org/10.1007/s00234-021-02802-y

30. Ye FQ, Berman KF, Ellmore T, Esposito G, van Horn JD, Yang Y et al (2000) H215O PET validation of steady-state arterial spin tagging cerebral blood flow measurements in humans.

Magn Reson Med 44:450–456. https://doi.org/10.1002/1522-2594(200009)44:3%3C450::aid-mrm16%3E3.0.co;2-0

31. Iida H, Itoh H, Nakazawa M, Hatazawa J, Nishimura H, Onishi Y et al (1994) Quantitative mapping of regional cerebral blood flow using iodine-123-IMP and SPECT. J Nucl Med 35:2019–2030

32. Mutsaerts HJ, van Dalen JW, Heijtel DF, Groot PF, Majoie CB, Petersen ET et al (2015) Cerebral perfusion measurements in Elderly with Hypertension using arterial spin labeling. PLoS ONE 10:e0133717. https://doi.org/10.1371/journal.pone.0133717

33. Fischl B (2012) FreeSurfer Neuroimage 62:774–781. https://doi.org/10.1016/j.neuroimage.2012.01.021

34. Jenkinson M, Beckmann CF, Behrens TE, Woolrich MW, Smith SM (2012) Fsl Neuroimage 62:782–790. https://doi.org/10.1016/j.neuroimage.2011.09.015

35. Nemoto K, Dan I, Rorden C, Ohnishi T, Tsuzuki D, Okamoto M et al (2011) Lin4Neuro: a customized Linux distribution ready for neuroimaging analysis. BMC Med Imaging 11:3. https://doi.org/10.1186/1471-2342-11-3

36. Iglesias JE, Billot B, Balbastre Y, Magdamo C, Arnold SE, Das S et al (2023) SynthSR: a public AI tool to turn heterogeneous clinical brain scans into high-resolution T1-weighted images for 3D morphometry. Sci Adv 9:eadd3607. https://doi.org/10.1126/sciadv.add3607

37. Yushkevich PA, Piven J, Hazlett HC, Smith RG, Ho S, Gee JC et al (2006) User-guided 3D active contour segmentation of anatomical structures: significantly improved efficiency and reliability. NeuroImage 31:1116–1128. https://doi.org/10.1016/j.neuroimage.2006.01.015

38. Kuroda S, Takigawa S, Kamiyama H, Abe H, Sakuragi M, Motomiya M et al (1990) [Diagnosis of hemodynamic compromise in patients with chronic cerebral ischemia; the detection of impaired vasodilatory capacity with 133Xe SPECT and acetazolamide (diamox) test]. No Shinkei Geka 18:167–173

39. Team Rc (2023) R: A Language and Environment for Statistical Computing

40. Group JS (2002) Japanese EC-IC bypass trial (JET study): study design and interim analysis. Surg Cereb Stroke 30:97–100. https://doi.org/10.2335/scs.30.97

41. Imaizumi M (2002) Detection of misery perfusion with split-dose 123I-iodoamphetamine single-photon emission computed tomography in patients with carotid occlusive diseases. Stroke 33:2217–2223

42. Nariai T, Suzuki R, Hirakawa K, Maehara T, Ishii K, Senda M (1995) Vascular reserve in chronic cerebral ischemia measured by the acetazolamide challenge test: comparison with positron emission tomography. AJNR Am J Neuroradiol 16:563–570

43. Widder B, Kleiser B, Krapf H (1994) Course of cerebrovascular reactivity in patients with carotid artery occlusions. Stroke 25:1963–1967. https://doi.org/10.1161/01.str.25.10.1963

44. Kuroda S, Shiga T, Ishikawa T, Houkin K, Narita T, Katoh C et al (2004) Reduced blood flow and preserved vasoreactivity characterize oxygen hypometabolism due to incomplete infarction in occlusive carotid artery diseases. J Nucl Med 45:943–949

45. Kuroda S, Kamiyama H, Abe H, Houkin K, Isobe M, Mitsumori K (1993) Acetazolamide test in detecting reduced cerebral perfusion reserve and predicting long-term prognosis in patients with internal carotid artery occlusion. Neurosurgery 32: 912–918; discussion 918–919. https://doi.org/10.1227/00006123-199306000-00005

46. Evans JD (1996) Straightforward statistics for the behavioral sciences. Thomson Brooks/Cole Publishing Co

47. Youden WJ (1950) Index for rating diagnostic tests. Cancer 3:32–35. https://doi.org/10.1002/1097-0142(1950)3:1%3C32::aid-cncr2820030106%3E3.0.co;2-3

48. Powers WJ (1991) Cerebral hemodynamics in ischemic cerebrovascular disease. Ann Neurol 29:231–240. https://doi.org/10.1002/ana.410290302

49. Kim JH, Lee SJ, Shin T, Kang KH, Choi PY, Kim JH et al (2000) Correlative assessment of hemodynamic parameters obtained with T2*-weighted perfusion MR imaging and SPECT in symptomatic carotid artery occlusion. AJNR Am J Neuroradiol 21:1450–1456

50. Lyu J, Ma N, Liebeskind DS, Wang DJJ, Ma L, Xu Y et al (2016) Arterial spin labeling magnetic resonance imaging estimation of Antegrade and collateral Flow in Unilateral Middle cerebral artery stenosis. Stroke 47:428–433. https://doi.org/10.1161/STROKEAHA.115.011057

51. Zaharchuk G, Do HM, Marks MP, Rosenberg J, Moseley ME, Steinberg GK (2011) Arterial spin-labeling MRI can identify the presence and intensity of collateral perfusion in patients with moyamoya disease. Stroke 42:2485–2491. https://doi.org/10.1161/STROKEAHA.111.616466

52. Dai W, Fong T, Jones RN, Marcantonio E, Schmitt E, Inouye SK et al (2017) Effects of arterial transit delay on cerebral blood flow quantification using arterial spin labeling in an elderly cohort. J Magn Reson Imaging 45:472–481. https://doi.org/10.1002/jmri.25367